Plant Physiology®

Plant Physiology, 2025, **199**, kiaf499
https://doi.org/10.1093/plphys/kiaf499
Advance access publication 5 November 2025
Letter

High-throughput genetic transformation and genome editing in pearl millet (*Pennisetum glaucum* L.)

V. Mohan Murali Achary,[1] L. Ruben B. Hernandez,[1] Huirong Gao,[2] Ning Wang,[2] Ana I. R. Castillo,[1] Todd Jones,[2] Sarah J. Hearne,[1] Anindya Bandyopadhyay[1,*]

[1]International Maize and Wheat Improvement Center (CIMMYT), Genetic Resources Program, Mexico-Veracruz, El Batan Km. 45, 56237, Texcoco, Mexico
[2]Corteva Agriscience, 7000 NW 62nd Ave, Johnston, IA 50131, USA
*Author for correspondence: a.bandyopadhyay@cgiar.org
The author responsible for distribution of materials integral to the findings presented in this article in accordance with the policy described in the Instructions for Authors (https://academic.oup.com/plphys/pages/General-Instructions) is: Anindya Bandyopadhyay, CIMMYT (a.bandyopadhyay@cgiar.org).

Dear Editor,

Pearl millet (*Pennisetum glaucum* L.), a C4 grass, accounts for 50% of total millet area in terms of global production (Ramu et al. 2023). It plays an important role in food and nutritional security for more than 90 million people in arid regions of Sub-Saharan Africa and Asia (Yadav et al. 2021). This crop exhibits an inherent capacity to adapt to drought and elevated temperatures, displaying resilience against saline and acidic soil conditions, rendering it particularly well-suited for utilization in marginal lands with low fertility. Pearl millet is gaining recognition as a critical alternative crop for food, animal feed, and fodder in numerous regions globally, including Australia, Brazil, Mexico, the United States, Canada, North Africa, and West and Central Asia (Yadav et al. 2021). It is gluten-free and has a low glycemic index. Additionally, it serves as a rich source of calcium, essential micronutrients such as iron and zinc, and a notable protein source. Genetic advancements in pearl millet have been relatively limited thus far, primarily achieved through breeding initiatives. Several agronomically important traits, including resistance to fungal diseases (downy mildew, blast, rust, smut, and ergot), tolerance to terminal drought, enhancements in grain and fodder quality, and reduced flour rancidity, have been recognized as crucial priorities from the farmers' perspective, thereby necessitating expedited genetic enhancement efforts in pearl millet (Yadav et al. 2021). Despite its significance as a climate-resilient crop for food and nutritional security, pearl millet has not received much focus for genetic improvement due to challenges associated with genetic transformation and in vitro regeneration. In the present work, we established an efficient genetic transformation and genome editing method in pearl millet using immature embryos, aided by morphogenic regulator (MR) genes and a helper plasmid.

To meet the growing global demand for grain, it is essential to leverage trait-specific genes through a blend of traditional and cutting-edge technological approaches, along with accelerated breeding efforts to develop new varieties. Genetic transformation and regeneration are essential steps in genome editing and transgenesis for gene functional assessment and crop trait enhancement. Monocots, particularly pearl millet, have historically posed challenges for genetic manipulation due to their recalcitrance to in vitro regeneration and resistance to *Agrobacterium tumefaciens*-mediated transformation which restricts the application of genome editing. Many studies have examined the in vitro regeneration of pearl millet, but genetic transformation research remains limited. Somatic embryogenesis-based regeneration systems in pearl millet have been reported using a range of explant sources including mature embryos/seed (Arockiasamy et al. 2006; Ramadevi et al. 2014), immature inflorescences (Goldman et al. 2003), immature zygotic embryo-derived calli (Girgi et al. 2006), shoot apices (Devi et al. 2000), scutellar tissue (Girgi et al. 2002), apical meristems (Goldman et al. 2003), leaf bases (Arockiasamy et al. 2006), embryogenic calli derived from shoot tips (Latha et al. 2006), and embryogenic cell suspensions (Tiécoura et al. 2015). Most of the aforementioned studies utilized particle bombardment for gene delivery and were prone to integration of multiple transgene copies, thought to contribute to transgene silencing in the progeny. Recently, the integration of developmental and MR genes into the transformation vector, coupled with virulent helper plasmids, has significantly improved the efficacy of *Agrobacterium*-mediated transformation and helped overcome the genotype-dependent transformation bottleneck in many recalcitrant crops (Lowe et al. 2016; Lee and Wang 2023).

In the present work, our transformation system is composed of 2 key components: a CRISPR/Cas9 knockout construct integrated with a combination of MRs and the *A. tumefaciens* strain carrying a helper plasmid. The CRISPR/Cas9 knockout construct has 3 components: 2 entry vectors and a binary vector compatible with the Gateway cloning system. The binary destination vector (DV; RV008586) contains a combination of the MR regulator genes *wuschel2* (*WUS2*) and *baby boom1* (*BBM1*), which were expressed independently under their respective promoters (Fig. 1A; Supplementary Fig. S1). The combined expression of the *Zea mays* transcription factors *WUS2* and *BBM1*, driven by auxin-inducible (*pAXIG*) and scutellum-specific (*pPLTP*) gene promoters in the transformation vector, has been shown to significantly promote somatic embryogenesis in various cereal crop species without exhibiting any detrimental pleiotropic effects in

Received March 25, 2025. Accepted July 21, 2025.

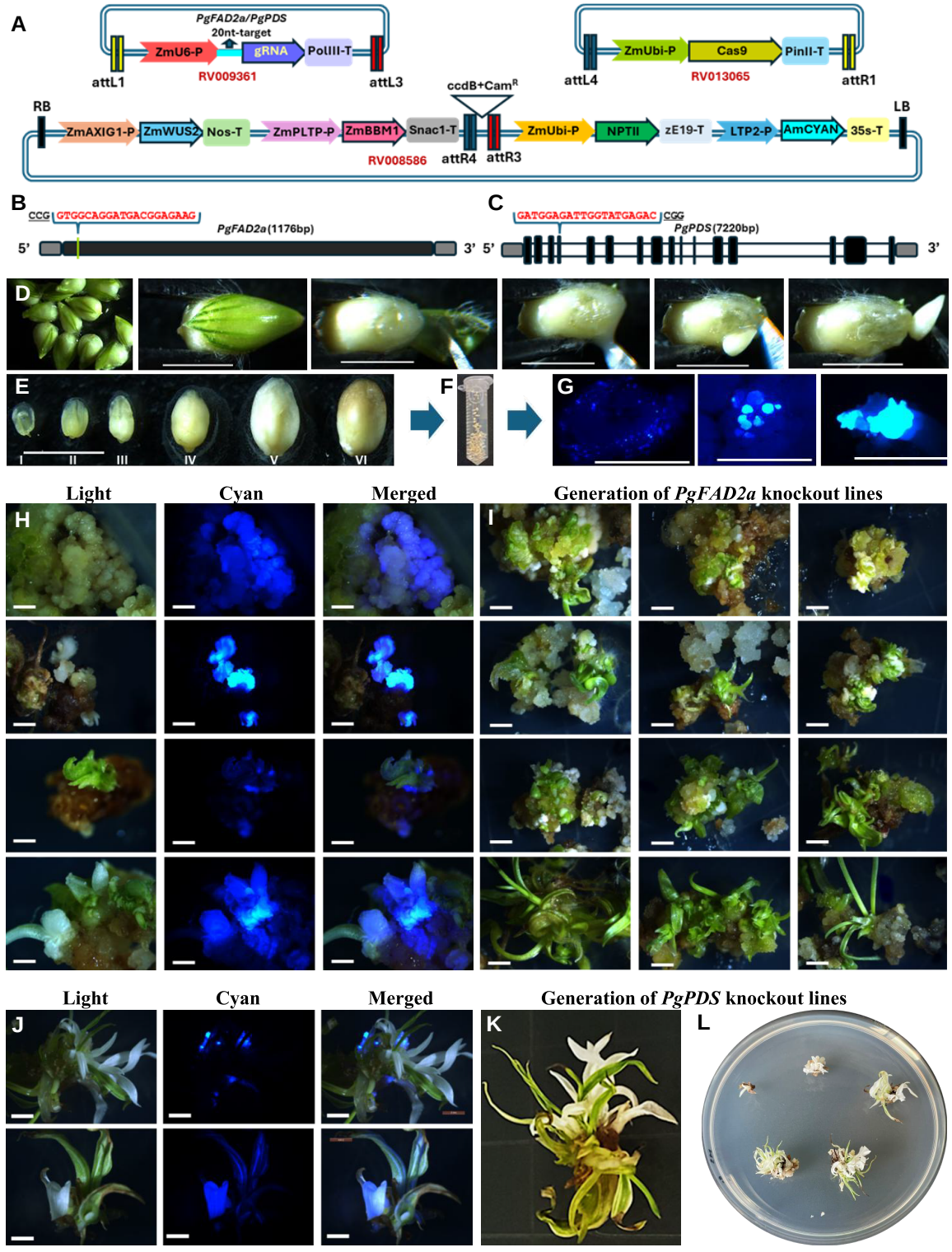

Figure 1. The figures represent genome editing vector constructs used, *fatty acid desaturase 2a* (*FAD2a*) and *phytoene desaturase* (*PDS*) gene structures, and tissue culture development of knockouts in pearl millet. **A)** Schematic representation of vector constructs used. The binary destination vector (DV; RV008586) harboring expression cassette of morphoregulator genes *WUS2* and *BBM1*, a visual fluorescent reporter gene *Anemonia majano CYAN* (*AmCYAN*), and a *neomycin phosphotransferase II* (*NPTII*) gene. The RV013065 entry vector contains the *Cas9* expression cassette under *Z. mays* polyubiquitin1 promoter (ZmUbi1P) and the entry vector RV009361 comprises a gRNA expression cassette under maize U6 promoter. **B)** The genomic architecture of *PgFAD2a* gene having single exon and location of sgRNA targeted region within the coding region of *PgFAD2a*. **C)** The genomic architecture of the *PgPDS* gene has 16 exons interrupted by 15 introns, and the sgRNA target region is within the 4th exon. **D)** Process of isolation of immature embryo following 2 wk post pollination from the developing pearl millet seeds. **E)** Different types of immature embryo. **F)** Collection of IEE in the infection medium. **G)** Expression of *AmCYAN* on the surface of IEE after 15 d of agroinfection. The subsequent figures in the same panel show development of secondary callus expressing *AmCYAN* in the selection medium. **H)** The figures illustrate the different stages of regeneration of the plant from the callus exhibiting *AmCYAN* expression. **I)** The figures illustrate the regeneration of plants from the transformed calli from the *PgFAD2a* knockout construct. **J to L)** Generation of *PgPDS* knockout plant showing white strip on the leaf surface. The scale bar represents 2 mm.

the transformed plants (Wang et al. 2023). It also includes a visual fluorescent reporter expression system *AmCYAN* that facilitates monitoring of the transformed cells during tissue culture, as well as an *NPTII* selection marker gene (Fig. 1A; Supplementary Fig. S1). The first entry vector (EV1; RV013065) contains the *Cas9* expression cassette driven by the robust maize polyubiquitin1 gene promoter (*ZmUbi1P*), while the second entry vector (EV2; RV009361) comprises a gRNA expression cassette under the regulation of the maize U6 promoter (Fig. 1A; Supplementary Fig. S1). The *Pennisetum glaucum fatty acid desaturase 2a* (*PgFAD2a*) genomic clones were amplified from different pearl millet varieties and Sanger sequenced (Supplementary Figs. S2 and S3 and Table S1). To generate the knockout construct, a highly specific single-guide RNA (sgRNA) target site was selected within the *PgFAD2a* genomic sequence, located near the 5′ end, 10 base pairs downstream of the start codon (ATG), on the antisense strand of the coding sequence (Fig. 1B; Supplementary Fig. S2). Similarly, for *Pennisetum glaucum phytoene desaturase* (*PgPDS*) knockout, a specific 20nt sgRNA target sequence was selected in the 4th exon of the *PgPDS* gene (Fig. 1C; Supplementary Figs. S4 and S5 and Table S1). The sgRNA duplex was cloned into the *Bbs*I restriction sites of the RV009361 vector, and its integration was verified through Sanger sequencing (Supplementary Fig. S6). The recombinant knockout vectors were developed following LR Gateway recombination cloning method (Invitrogen, United States) and further confirmed by PCR and whole plasmid sequencing (Supplementary Materials and Methods and Table S1). The recombinant vector was transformed into *Agrobacterium* (LBA4404) harboring the helper plasmid (V001832), which was then used for pearl millet transformation (Supplementary Fig. S7). The isolated immature embryos (IIEs) of the pearl millet genotype (IKMB18002), harvested approximately 2 wk after pollination, were used for *Agrobacterium*-mediated transformation (Fig. 1D; Supplementary Materials and Methods). For the transformation, we used Types IV and V immature embryos, which resulted in a high frequency of callus induction (Fig. 1E). The use of these immature embryo types allowed us to achieve a robust and efficient callus induction process, as observed in our previous study. The IIE explants were coincubated for 20 min with the *Agrobacterium* suspension harboring either the *PgFAD2a*- or *PgPDS*-knockout DNA constructs, with intermittent vortex agitation (1 × 5 to 10 s at 200 rpm) (Fig. 1F). The explants were transferred to the cocultivation solid media (562 V) and incubated in the presence of 100 μM acetosyringone for 48 h in the dark to facilitate infection (Supplementary Materials and Methods, Supplementary Table S2). Two weeks after *Agrobacterium* transformation in the resting medium (605T), we observed CYAN-fluorescent spots on the IIE, indicating successful integration of the T-DNA and robust expression of the *AmCYAN* reporter gene (Fig. 1G). The actively growing calli after 25 d in resting media were transferred into selection medium (605A) containing 50 mg/L G418 antibiotic and allowed to grow for 3 wk in the dark until the callus reached a size of approximately 0.5 to 0.8 mm (Fig. 1G). The G418 antibiotic selected callus was transferred to regeneration media (M20) and exposed to light (12 h dark–light cycle) until the formation of young plantlets (Fig. 1, H and I; Supplementary Materials and Methods and Table S2). Following 2 to 3 wk in the regeneration, the young plantlets were transferred into rooting media (M51) for 25 d to promote root development (Supplementary Fig. S8) and subsequently into soil pots under greenhouse conditions maintained at 26 °C with 45% relative humidity (Supplementary Fig. S9). The *PgPDS* edited plants displayed a distinct chlorophyll bleach stripped albino appearance in the regeneration medium (Fig. 1, J to L; Supplementary Fig. S8A). Figure 2, A to L describes the details of editing of *PgFAD2a* and *PgPDS* and timeline of timeline of pearl millet transformation. We achieved a secondary callus induction frequency of 10% to 30% in the G418 medium (Fig. 2H). Furthermore, our analysis indicated that in most batches, approximately 90% to 97% (calculated based on the number of plants produced) of the putative T0 transformed plants generated through tissue culture had *Cas9* gene integration confirmed by PCR analysis (Supplementary Fig. S10). Additionally, we developed long primer pairs flanking the *PgFAD2a* gene target region for assessing the frequency of diverse long insertions and deletions, as well as the editing efficiency of CRISPR/Cas9 system (Supplementary Table S1 and Fig. S11). Sanger sequencing analysis revealed a high rate of indel editing, ranging from 78% to 100% (for *PgFAD2a*; PMN25-PMN32) and 36% to 38% (for *PgPDS*; PMN41-PMN42), across various batches of *Cas9*-confirmed T0 plants. A possible explanation for the differential editing frequency between the genes *PgFAD2a* and *PgPDS* may be related to the effectiveness of the sgRNA sequences (Konstantakos et al. 2022). The number of homozygous, heterozygous, and biallelic mutations is presented in a tabulated form (Fig. 2H). Among the *PgFAD2a*-T0 edited lines, we identified that 6% to 25% of the plants were homozygous edits (HOZEs), with a single plant having a 13 base pair deletion and 2 additional plants with single base insertions in the target region (Fig. 2, A and B). Similarly, we also identified that 8% to 50% of the edited lines showed biallelic edits (BIEs), and 25% to 100% of the edited lines showed heterozygous edits (HEZEs), as confirmed by Sanger sequencing (Fig. 2H). Among the *PgPDS*-T0 edited lines, all plants showed heterozygous edits (Fig. 2, C and H). Furthermore, we observed that the T0 edited lines, carrying mutations in *PgFAD2a*, did not exhibit any noticeable phenotypic defects or abnormalities during the developmental stage, and we successfully obtained the seeds (Fig. 2, D to G; Supplementary Fig. S9). In contrast, the *PgPDS* edited lines exhibited albino phenotypes and delayed growth during the tissue culture regeneration process (Fig. 1, J to L; Supplementary Fig. S8A). To confirm the indel frequency among the edited lines for *PgFAD2a*, we utilized the popular ICE Analysis-v3.0 platform, which enabled us to analyze and quantify the different types of insertions and deletions within the heterozygous population. From the analysis, we notice that 4% showed wild-type genotype, 53.4% had different insertion mutations, and 36.9% had different types of deletion mutations (Fig. 2I). We conducted a detailed analysis and categorized various insertion and deletion mutations that ranged in length from 1 to 250 base pairs (Fig. 2, J and K). These findings indicate that the current genome editing system demonstrated robust editing outcomes and produced high frequencies of successful indel modifications in the pearl millet genome. The design of specific sgRNA and the robust expression of both the sgRNAs and the Cas9 enzyme are crucial factors that determine the high-frequency outcome of genome editing. Similarly, the utilization of efficient fluorescent marker system is also a key component in the present investigation for monitoring transformed cell and callus during the tissue culture process. Various visible marker systems have been employed in transformation studies across different crops, including the *RUBY* reporter in maize (Lee et al. 2023), the *GFP* fluorescent marker in diverse cereals (Wang et al. 2023), and the *dsRED* (Huai et al. 2023), *AmCYAN* (Wenck et al. 2003), FastRED (Castel et al. 2019), and *GUS* marker systems. The nondestructive fluorescent marker system has demonstrated greater efficacy and advantages in comparison to the *RUBY* reporter and *GUS* marker systems. Given that the majority of cultivated crops exhibit recalcitrance to genetic

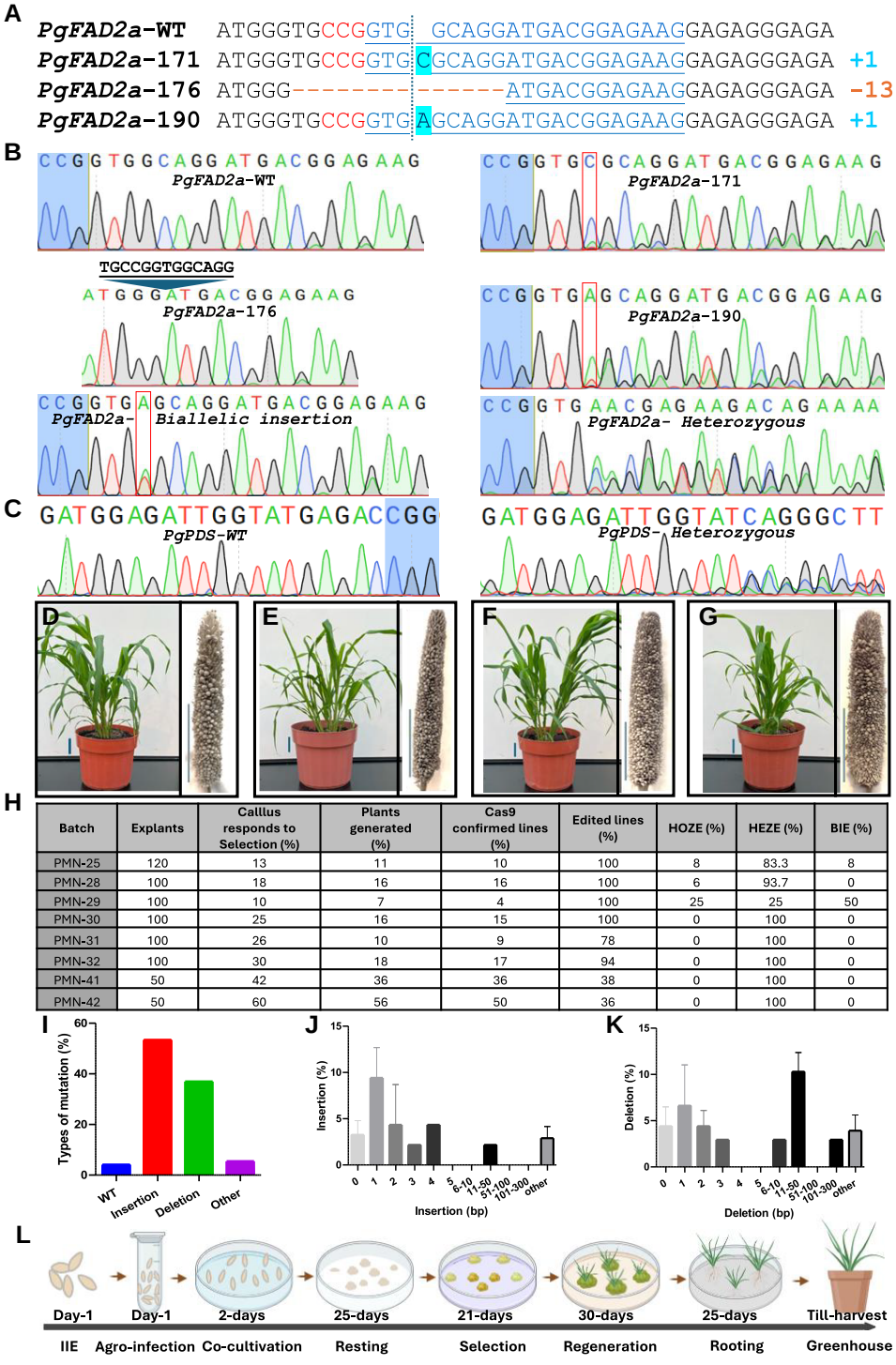

Batch	Explants	Calllus responds to Selection (%)	Plants generated (%)	Cas9 confirmed lines (%)	Edited lines (%)	HOZE (%)	HEZE (%)	BIE (%)
PMN-25	120	13	11	10	100	8	83.3	8
PMN-28	100	18	16	16	100	6	93.7	0
PMN-29	100	10	7	4	100	25	25	50
PMN-30	100	25	16	15	100	0	100	0
PMN-31	100	26	10	9	78	0	100	0
PMN-32	100	30	18	17	94	0	100	0
PMN-41	50	42	36	36	38	0	100	0
PMN-42	50	60	56	50	36	0	100	0

Figure 2. Genotyping of *PgFAD2a* and *PgPDS* edited lines and timeline of pearl millet transformation. **A)** The nucleotide shows the homozygous insertion and deletion (INDEL) mutation profile of *PgFAD2a* targeted region among T0 lines. The vertical dotted line shows Cas9 cleavage on DNA strands 3 bases downstream of PAM. **B)** The chromatogram illustrates different types of editing including homozygous, biallelic, and heterozygous editing at the *PgFAD2a* target site. **C)** Sequencing of wild type (WT) plants and *PgPDS* edited lines revealed heterozygous chromatograms at the *PgPDS* target sites. **D to G)** The phenotype of different types of WT and edited lines of *PgFAD2a* grown in greenhouse conditions. **D)** Wild-type plant, **E)** PgFAD2a-171 plant with "C" insertion mutation, **F)** PgFAD2a-176 plant with 13 base deletion mutation, and **G)** PgFAD2a-190 plant with "A" insertion mutation. The plants and panicles were photographed at different times, and the scale bars in the figures represent 5 cm. **H)** The table summarizes the different transformation batches, transformation efficiency, editing frequency, and % of different types of edits. The abbreviations HOZE, HEZE, and BIE indicate homozygous edits, heterozygous edits, and biallelic edits, respectively. **I to K)** The graphs generated using ICE analysis demonstrate the percentage of insertions and deletions as well as the length of insertion and deletion frequency among the *PgFAD2a* T0 edited lines. The ratio of insertions and deletions was determined from T0-*PgFAD2a* population ($n = 80$). The figures for the length of insertion and deletion edited frequency represent the mean of T0-*PgFAD2a* population ± SD ($n = 46$) and ($n = 34$), respectively. **L)** The following figure depicts a graphical representation of a timeline illustrating the various stages and steps involved in the pearl millet transformation and generation of edited events through the tissue culture process (The diagram was created using BioRender.com.).

transformation, this restricts the genetic foundation available for trait enhancement. In the present investigation, the use of a combination of the *BBM1* and *WUS2* morphoregulatory genes within the destination vector assists in overcoming transformation challenges and facilitates the accelerated regeneration of transformed callus into a fully developed plant (Supplementary Fig. S1). Over the past several years, the deployment of diverse MR genes, such as *AGAMOUS-LIKE* (*AGL*), *GROWTH-REGULATING FACTORS* (*GRFs*), *GRF-INTERACTING FACTORS* (*GIFs*), *WUSCHEL* (*WUS*), *BABYBOOM* (*BBM*), *LEAFY COTYLEDON (LEC)*, *WUSCHEL-RELATED HOMEOBOX (WOXs)*, *SHOOT MERISTEMLESS* (*STM*), *CUP-SHAPED COTYLEDON* (*CUC*), *ENHANCER OF SHOOT REGENERATION* (*ESR*), *PLETHORA* (*PLTs*), and *ISOPENTENYL TRANSFERASE* (*IPT*), either independently or in combination, has markedly increased transformation efficiency and facilitated the reprogramming of transformed explants into the processes of somatic embryogenesis or organogenesis across numerous crop species that were historically resistant to genetic transformation (Duan et al. 2022; Lee and Wang 2023; Belaffif et al. 2025). It has been observed that strong overexpression of certain MR genes resulted in an abnormal or aberrant phenotype (Lee and Wang 2023). The current study utilized a similar approach to increase the transformation rate while avoiding aberrant phenotypes.

In summary, we have successfully developed a streamlined and efficient *Agrobacterium*-mediated transformation and genome editing system for recalcitrant pearl millet genotype. The entire transformation process, starting from the use of IIE as an explant for transformation, culminated in the development of a complete plant within a timeframe of 145 d (Fig. 2L). The MR components of the transformation system can potentially surmount the genotypic dependence of genetic transformation in pearl millet cultivars, offering substantial potential for functional genomics investigations, genome editing, and crop enhancement in other elite pearl millet cultivars. Although we employed a single sgRNA for genome editing, we achieved a high rate of on-target editing efficiency (78% to 100%) in the *PgFAD2a* gene. Furthermore, the utilization of the *AmCYAN* fluorescent marker facilitated the identification of transformants across various developmental stages of pearl millet tissues, demonstrating its effectiveness as a nondestructive fluorescent marker for crop transformation and also significantly decreased the nontransformed plant escape rates. The integration of this marker into the genome editing vector system can also facilitate the screening of transgenic plants or the identification of transgene-free segregants. The present genome editing system, featuring robust expression of the *Cas9* and sgRNA components along with a helper plasmid, can establish a highly efficient platform for precision genetics to generate targeted genome modifications in other elite pearl millet germplasm for trait improvement.

Acknowledgments

The authors would like to thank Dr. Lava Kumar, IITA, Kenya, for sharing pearl millet genotype (ICMB93333-I, ICMB93333-BF, ICMB187333, ICMB177004, ICMB177002, and IKMB18002) seeds.

Author contributions

A.B., S.J.H., and T.J. conceptualized the study. V.M.M.A. and L.R.B.H. established the pearl millet transformation protocol. V.M.M.A., A.B., S.J.H., and T.J. wrote, revised, and finalized the manuscript. H.G., N.W., and T.J. developed the base vector systems used in the study. A.I.R.C. and V.M.M.A. performed molecular analyses. V.M.M.A. developed knockout vector constructs and analyzed the data. All authors read and approved the manuscript.

Supplementary data

The following materials are available in the online version of this article.

Supplementary Materials and Methods

Supplementary Figure S1. Detailed vector maps of the RV009361, RV013065, and RV008586 expression plasmids.

Supplementary Figure S2. Coding sequence of *PgFAD2a* gene and location of sgRNA.

Supplementary Figure S3. Amplification of *PgFAD2a* full-length genes from the pearl millet genotypes.

Supplementary Figure S4. Coding sequence of *PgPDS* gene and location of sgRNA.

Supplementary Figure S5. The *PgPDS* genomic region targeted for the knockdown study.

Supplementary Figure S6. The assembly of the sgRNA primer duplex into the RV009361 vector.

Supplementary Figure S7. Vector map of V001832 (pPHP71539) expression plasmids.

Supplementary Figure S8. Tissue culture generation of *PgPDS* and *PgFAD2a* knockout plants.

Supplementary Figure S9. Tissue culture-generated *PgFAD2a* knockout plants maintained under greenhouse conditions.

Supplementary Figure S10. PCR confirmation of T0 putative plants developed from the *PgFAD2a* knockout vector.

Supplementary Figure S11. Amplification of the *PgFAD2a* target region from the T0 putative plants.

Supplementary Table S1. List of primers used in the present study.

Supplementary Table S2. Details of media composition used in the tissue culture generation of knockout lines.

Funding

The research was supported by grants from the Gates Foundation (Grant number INV-039460).

Conflict of interest statement. The authors declare no conflict of interest.

Data availability

The data that supports this article can be found in the paper as well as in its online Supplementary material. The plasmids used in this study were obtained from Corteva Agriscience under a material transfer agreement with CIMMYT.

References

Arockiasamy S, Rani SS, Ignacimuthu S, Melchias G. Efficient protocols for in vitro regeneration of *Pennisetum glaucum* (L.). Br. *Indian J Exp Biol*. 2006:44(9):757–761.

Belaffif MB, Brown MC, Marcial B, Baysal C, Swaminathan K. New strategies to advance plant transformation. *Curr Opin Biotechnol*. 2025:91:103241. https://doi.org/10.1016/j.copbio.2024.103241

Castel B, Tomlinson L, Locci F, Yang Y, Jones JDG. Optimization of T-DNA architecture for Cas9-mediated mutagenesis in *Arabidopsis*. *PLoS One*. 2019:14(1):e0204778. https://doi.org/10.1371/journal.pone.0204778

Devi P, Zhong H, Sticklen MB. In vitro morphogenesis of pearl millet [*Pennisetum glaucum* (L.) R.Br.]: efficient production of multiple shoots and inflorescences from shoot apices. *Plant Cell Rep*. 2000:19(6):546–550. https://doi.org/10.1007/s002990050771

Duan H, Maren NA, Ranney TG, Liu W. New opportunities for using WUS/BBM and GRF-GIF genes to enhance genetic transformation of ornamental plants. *Ornamental Plant Res*. 2022:2(1):4. https://doi.org/10.48130/OPR-2022-0004

Girgi M, Breese WA, Lorz H, Oldach KH. Rust and downy mildew resistance in pearl millet (*Pennisetum glaucum*) mediated by heterologous expression of the afp gene from *Aspergillus giganteus*. *Transgenic Res*. 2006:15(3):313–324. https://doi.org/10.1007/s11248-006-0001-8

Girgi M, O'Kennedy MM, Morgenstern A, Smith G, Lorz H, Oldach KH. Transgenic and herbicide resistant pearl millet (*Pennisetum glaucum* L.) R.Br. via microprojectile bombardment of scutellar tissue. *Mol Breed*. 2002:10(4):243–252. https://doi.org/10.1023/A:1020558315265

Goldman JJ, Hanna WW, Fleming G, Ozias-Akins P. Fertile transgenic pearl millet [*Pennisetum glaucum* (L.) R. Br.] plants recovered through microprojectile bombardment and phosphinothricin selection of apical meristem-, inflorescence-, and immature embryo-derived embryogenic tissues. *Plant Cell Rep*. 2003:21(10):999–1009. https://doi.org/10.1007/s00299-003-0615-8

Huai D, Wu J, Xue X, Hu M, Zhi C, Pandey MK, Liu N, Huang L, Bai D, Yan L, *et al*. Red fluorescence protein (DsRed2) promotes the screening efficiency in peanut genetic transformation. *Front Plant Sci*. 2023:14:1123644. https://doi.org/10.3389/fpls.2023.1123644

Konstantakos V, Nentidis A, Krithara A, Paliouras G. CRISPR-Cas9 gRNA efficiency prediction: an overview of predictive tools and the role of deep learning. *Nucleic Acids Res*. 2022:50(7):3616–3637. https://doi.org/10.1093/nar/gkac192

Latha MA, Rao KV, Reddy TP, Reddy VD. Development of transgenic pearl millet (*Pennisetum glaucum* (L.) R. Br.) plants resistant to downy mildew. *Plant Cell Rep*. 2006:25(9):927–935. https://doi.org/10.1007/s00299-006-0141-6

Lee K, Kang M, Ji Q, Grosic S, Wang K. New T-DNA binary vectors with NptII selection and RUBY reporter for efficient maize transformation and targeted mutagenesis. *Plant Physiol*. 2023:192(4):2598–2603. https://doi.org/10.1093/plphys/kiad231

Lee K, Wang K. Strategies for genotype-flexible plant transformation. *Curr Opin Biotechnol*. 2023:79:102848. https://doi.org/10.1016/j.copbio.2022.102848

Lowe K, Wu E, Wang N, Hoerster G, Hastings C, Cho MJ, Scelonge C, Lenderts B, Chamberlin M, Cushatt J, *et al*. Morphogenic regulators baby boom and Wuschel improve monocot transformation. *Plant Cell*. 2016:28(9):1998–2015. https://doi.org/10.1105/tpc.16.00124

Ramadevi R, Rao KV, Reddy VD. *Agrobacterium tumefaciens* mediated genetic transformation and production of stable transgenic pearl millet (*Pennisetum glaucum* [L.] R. Br.). *Vitro Cell Dev Biol Plant*. 2014:50(4):392–400. https://doi.org/10.1007/s11627-013-9592-y

Ramu P, Srivastava RK, Sanyal A, Fengler K, Cao J, Zhang Y, Nimkar M, Gerke J, Shreedharan S, Llaca V, *et al*. Improved pearl millet genomes representing the global heterotic pool offer a framework for molecular breeding applications. *Commun Biol*. 2023:6(1):902. https://doi.org/10.1038/s42003-023-05258-3

Tiécoura K, Kouassi AB, Oulo NA, Bi SG, Dinant M, Ledou L. In vitro transformation of pearl millet (*Pennisetum glaucum* (L). R. BR.): selection of chlorsulfuron-resistant plants and long term expression of the gus gene under the control of the emu promoter. *Afr J Biotechnol*. 2015:14(46):3112–3123. https://doi.org/10.5897/AJB2015.14983

Wang N, Ryan L, Sardesai N, Wu E, Lenderts B, Lowe K, Che P, Anand A, Worden A, van Dyk D, *et al*. Leaf transformation for efficient random integration and targeted genome modification in maize and sorghum. *Nat Plants*. 2023:9(2):255–270. https://doi.org/10.1038/s41477-022-01338-0

Wenck A, Pugieux C, Turner M, Dunn M, Stacy C, Tiozzo A, Dunder E, van Grinsven E, Khan R, Sigareva M, *et al*. Reef-coral proteins as visual, non-destructive reporters for plant transformation. *Plant Cell Rep*. 2003:22(4):244–251. https://doi.org/10.1007/s00299-003-0690-x

Yadav OP, Gupta SK, Govindaraj M, Sharma R, Varshney RK, Srivastava RK, Rathore A, Mahala RS. Genetic gains in pearl millet in India: insights into historic breeding strategies and future perspective. *Front Plant Sci*. 2021:12:645038. https://doi.org/10.3389/fpls.2021.645038